Role of transvaginal sonography and magnetic resonance imaging in the diagnosis of uterine adenomyosis

Marc Bazot, M.D.[a,b] and Emile Daraï, M.D., Ph.D.[b,c,d]

[a] Department of Radiology, Tenon Hospital, Assistance Publique des Hôpitaux de Paris, Université Pierre et Marie Curie Paris 6, Paris; [b] Groupe de Recherche Clinique GRC6-UPMC, Centre Expert En Endométriose (C3E), Paris; [c] Department of Obstetrics and Gynecology, Assistance Publique des Hôpitaux de Paris, Université Pierre et Marie Curie Paris; and [d] Inserm UMRS-938, Paris, France

The aim of the present review, conducted according to PRISMA statement recommendations, was to evaluate the contribution of transvaginal sonography (TVS) and magnetic resonance imaging (MRI) to diagnose adenomyosis. Although there is a lack of consensus on adenomyosis classification, three subtypes are described, internal, external adenomyosis, and adenomyomas. Using TVS, whatever the subtype, pooled sensitivities, pooled specificities, and pooled positive likelihood ratios are 0.72–0.82, 0.85–0.81, and 4.67–3.7, respectively, but with a high heterogeneity between the studies. MRI has a pooled sensitivity of 0.77, specificity of 0.89, positive likelihood ratio of 6.5, and negative likelihood ratio of 0.2 for all subtypes. Our results suggest that MRI is more useful than TVS in the diagnosis of adenomyosis. Further studies are required to determine the performance of direct signs (cystic component) and indirect signs (characteristics of junctional zone) to avoid misdiagnosis of adenomyosis. (Fertil Steril® 2018;109:389–97. ©2018 by American Society for Reproductive Medicine.)

Key Words: Adenomyosis, endometriosis, transvaginal sonography, magnetic resonance imaging, internal adenomyosis

Discuss: You can discuss this article with its authors and other readers at https://www.fertstertdialog.com/users/16110-fertility-and-sterility/posts/29413-25402

Uterine adenomyosis is a benign condition defined by the presence of endometrial glands and stroma within the myometrium (1). Although the prevalence of uterine adenomyosis is unknown, it is usually diagnosed in multiparous women experiencing bleeding or pelvic pain, mainly during the late reproductive period (2–4). However, the increasing use of ultrasonography (US) and magnetic resonance imaging (MRI) in women with chronic pelvic pain or infertility has contributed to the detection of adenomyosis in younger women, suggesting several etiopathogenic conditions and different subtypes.

While there is a lack of consensus about the pathogenesis of adenomyosis, various risk factors have been identified and possible etiopathogenic pathways include alteration in endometrial function, a mechanism of tissue injury and repair, and a theory involving stem cells (5–7).

Recent advances in imaging techniques have had an impact on the detection of uterine adenomyosis (8–12) and imaging criteria are now part of the diagnostic workup along with histopathological features (9–12). However, because previously published imaging data are insufficient to distinguish between the subtypes of adenomyosis, there is a need for uniform terminology and consensus classification (13). The aims of this review are to clarify the definition of adenomyosis and to determine the value of the various US and MRI criteria used in the diagnosis of the various subtypes of adenomyosis.

METHODS

The review was carried out in accordance with the PRISMA statement recommendations for reviews and meta-analysis. The literature search was conducted in MEDLINE, Embase, and the Cochrane Library and was limited to studies published in English and French between 1979 and 2017. The MeSH Database of PubMed helped steer the search by combining the MeSH key words: adenomyosis, uterine adenomyosis, adenomyomas with the terms imaging, transvaginal sonography, ultrasound, MRI, or magnetic resonance imaging. To ensure the relevance of the publications retrieved, additional inclusion criteria were applied. To be included, the published studies had to contain a clear description of the imaging technique. Furthermore, papers describing imaging techniques used to treat adenomyosis were excluded.

Received December 5, 2017; revised January 15, 2018; accepted January 18, 2018.
M.B. has nothing to disclose. E.D. has nothing to disclose.
Correspondence: Marc Bazot, M.D., Department of Radiology, Hôpital Tenon, 4 rue de La Chine, Paris 75020, France (E-mail: marc.bazot@aphp.fr).

Fertility and Sterility® Vol. 109, No. 3, March 2018 0015-0282/$36.00

https://doi.org/10.1016/j.fertnstert.2018.01.024

Redundant articles were removed after an initial selection, and other articles were then removed if their title, abstract, or material and methods did not fit the objective of our review. Finally, after reading the remaining studies, we eliminated those that did not provide clear data on the diagnosis of adenomyosis, as well as those assessing the same series of women. Of the 741 articles selected initially, 687 were excluded based on title and abstract. For this review, 57 articles were used.

CLASSIFICATION OF ADENOMYOSIS

Adenomyosis was initially described in 1860 by Rokitansky (14) as fibrous tumors containing gland-like structures that resemble endometrial glands. In 1920, Thomas Cullen (15) published a preliminary report on adenomyoma uteri diffusum benignum and on the distribution of adenomyomas containing uterine mucosa. He suggested that diffuse adenomyoma was the result of basal endometrial invasion and that an encapsulated variety was possibly of müllerian origin (15).

In 1921, Sampson put forward that adenomyoma of the uterus could be differentiated into three groups according to the origin: the first when the growth arises from an invasion of the uterine wall by the mucosa lining (invasion from within the uterus); the second with the growth arising from the serous surface by endometrial tissue from an endometrial cyst (invasion from without the uterus); and the third arising from misplaced endometrial tissue in the uterine wall (16).

In 2012, Kishi et al. (17) differentiated uterine adenomyosis into four subtypes based on MRI analysis: subtype I consists of adenomyosis occurring in the uterine inner layer without affecting the outer structures; subtype II of adenomyosis occurring in the uterine outer layer without affecting the inner structures; subtype III of adenomyosis occurring alone unrelated to structural components; and subtype IV composed of adenomyosis that did not satisfy these criteria (17).

We recently suggested a classification of adenomyosis according to MRI features which allows us to distinguish between internal adenomyosis, external adenomyosis and structural-related adenomyoma subtypes with a potential relation for therapeutic strategy (Table 1, Fig. 1) (18). Internal, external adenomyosis, and adenomyomas can be present alone or in association in this model. Current classification proposals and future perspectives are discussed more extensively by Gordts et al. (19) in this issue.

ULTRASONOGRAPHY AND ADENOMYOSIS

The diagnosis of adenomyosis was initially based on transabdominal US (TUS) criteria (11, 20, 21). This technique can visualize a big, regular, heterogeneous uterus containing tiny cystic lesions of 2–7 mm (20). TUS is useful in patients with bleeding or dysmenorrhea to detect uterine leiomyomas or endometrial disorders. In a study including 129 patients undergoing hysterectomy for bleeding and examined by TUS, the prevalence of adenomyosis in women with and without uterine leiomyomas or endocavitary abnormalities was 24.5% and 91.3%, respectively (22). Despite a high specificity (97%–97.5%), TUS had a low sensitivity (30%–63%) due to its limited image resolution (11, 21). However, as TUS is unable to distinguish between the various subtypes of adenomyosis, transvaginal sonography (TVS) should always be used for the detection of adenomyosis.

Transvaginal Sonography and Internal Adenomyosis

Examination by TVS constitutes an acceptable, moderately accurate and minimally invasive first-line test to detect internal adenomyosis (23) (Table 2). A very detailed description of

TABLE 1

Classification of adenomyosis.

Adenomyosis subtype	Definition	Figure
Internal adenomyosis (Ai)		
Focal adenomyosis (Ai0)	Localized intramyometrial tiny cystic component with or without JZ bulging (unique or multiple)	1A
Superficial adenomyosis (Ai1)	Disseminated subendometrial tiny cystic component without JZ hypertrophy (symmetric or asymmetric)	1B, 1C
Diffuse adenomyosis (Ai2)	Disseminated intramyometrial tiny cystic component with JZ hypertrophy (symmetric or asymmetric)	1D, 1E
Adenomyomas (Ad)		
Intramural solid adenomyoma (Ad1)	Ill-defined myometrial lesion with tiny cystic component (hemorrhagic or not)	1F
Intramural cystic adenomyoma (Ad2)	Ill-defined myometrial lesion with hemorrhagic cystic cavity	1G
Submucosal adenomyoma (Ad3)	Ill-defined myometrial lesion with tiny cystic component and intracavitary protrusion	1H
Subserosal adenomyoma (Ad4)	Ill-defined subserous myometrial lesion with tiny cystic component	1I
External adenomyosis (Ae)		
Posterior external adenomyosis (Ae1)	Ill-defined subserosal posterior myometrial mass associated with posterior deep endometriosis	1J
Anterior external adenomyosis (Ae2)	Ill-defined subserosal anterior myometrial mass associated with anterior deep endometriosis	1K

Note: asymmetric = predominant disseminated involvement by adenomyosis in one uterine wall; JZ = junctional zone; symmetric = disseminated involvement by adenomyosis in anterior and posterior uterine wall.

Bazot. Adenomyosis and imaging techniques. Fertil Steril 2018.

FIGURE 1

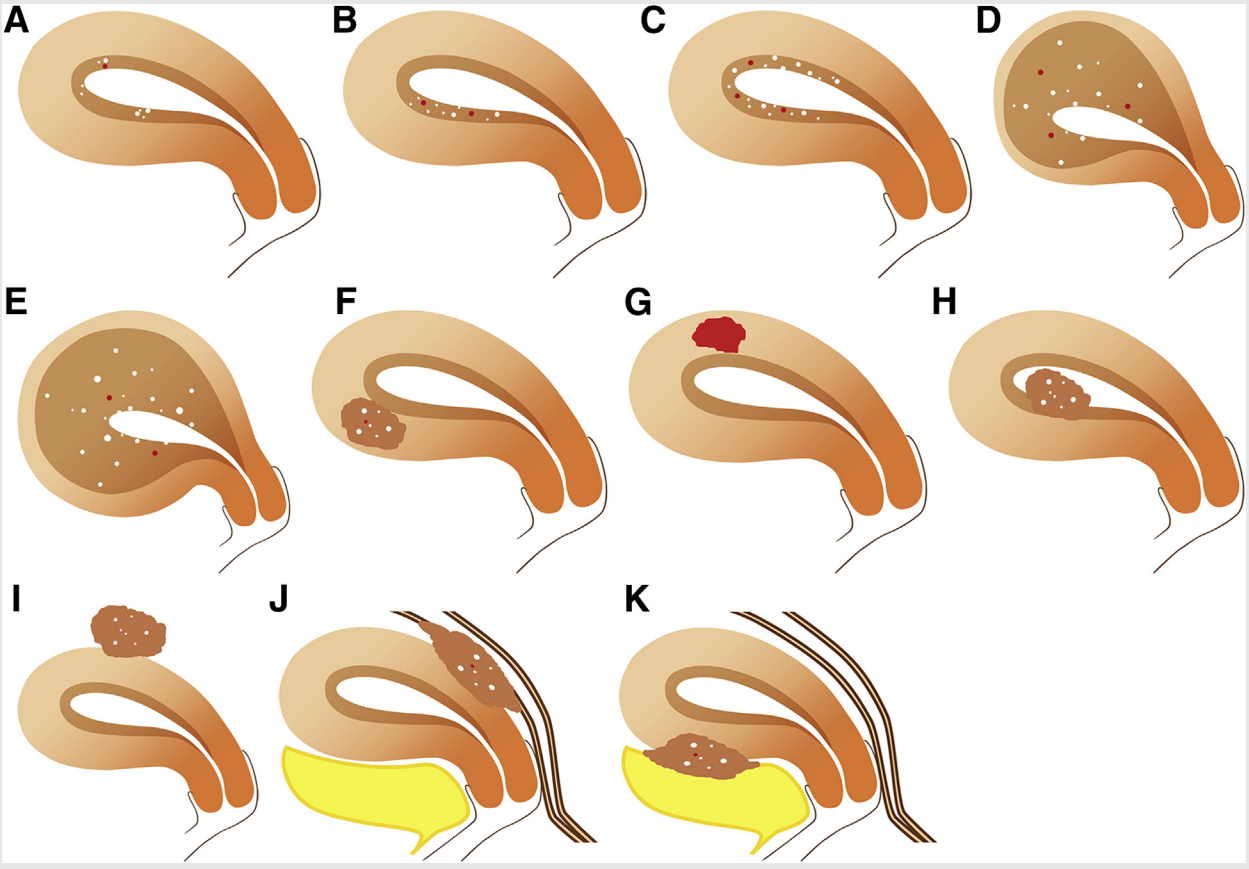

Magnetic resonance imaging classification of adenomyosis: different morphologic and locations of adenomyosis subtypes including internal adenomyosis, adenomyomas, and external adenomyosis. (**A**) Internal adenomyosis comprised focal or multifocal adenomyosis, (**B**) superficial asymmetric or (**C**) symmetric adenomyosis, and (**D**) diffuse asymmetric or (**E**) symmetric adenomyosis. Adenomyomas are related to intramural adenomyoma, (**F**) solid or (**G**) cystic and (**H**) submucosal or (**I**) subserosal adenomyomas. External adenomyosis are represented by (**J**) posterior adenomyosis and (**K**) anteriorassociated respectively with posterior and anterior deep endometriosis. (Modified from Bazot [18]. Pathologie Myométriale. Imagerie de la femme. Lavoisier; 2018).

Bazot. Adenomyosis and imaging techniques. Fertil Steril 2018.

the ultrasound findings for adenomyosis was provided recently by Van den Bosch et al. (24).

Several direct features are related to the presence of endometrial tissue within the myometrium (10). Tiny myometrial cysts (2 mm–9 mm) corresponding to cystic or hemorrhagic endometrial glands, mainly located in the superficial myometrium, are highly specific (98%), but of low sensitivity (50%–65%) (Fig. 2A and B) (10, 22, 25–28). Non-cystic endometrial tissue gives rise to hyperechoic nodules or striations, of irregular or nodular aspect, or poor definition of the endometrial-myometrial interface (10, 27).

Indirect features are related to hypertrophic myometrial reaction (10). Diffuse myometrial heterogeneity is common and has a high sensitivity (80.8%–100%), but low specificity (30%–65%) (22, 26, 28). Associated thin hypoechoic linear striations within a heterogeneous myometrium reinforce the diagnosis of internal adenomyosis, this criterion being of low sensitivity (3.8%–66.6%), but high specificity (90%–98.7%) (Fig. 2B) (22, 26, 28). These hypoechoic linear striations are easily detected in the absence of leiomyomas and during the reproductive age (22).

Diffuse asymmetric or symmetric widening of the myometrial wall(s) is secondary to myometrial hypertrophy and mainly related to deep diffuse internal adenomyosis. All but one of the TVS studies evaluating the depth of penetration within the myometrium found a low correlation with histopathology (11, 26, 29, 30). Atri et al. (10) found a good correlation but their study was performed on gross specimens.

Several studies exploring the role of TVS in the diagnosis of adenomyosis report discrepant results (10, 11, 29). These discrepancies can partly be explained by the clinical, US and histopathologic criteria used. The main differential diagnosis of adenomyosis is the association with uterine leiomyomas (with a coexistence of 40%) and represents one of the main limits of TVS.

Three recent meta-analyses used the Quality Assessment of Diagnostic Accuracy Studies criteria to evaluate the imaging quality (23, 31, 32). Descriptive analysis found pooled

TABLE 2

References providing descriptive analysis of adenomyosis in accordance with subtype.

Reference	Subtype	Prev (%)	Sens (%)	Spec (%)	PPV (%)	NPV (%)	PLR	NLR
Ultrasound								
Fedele et al. 1992 (25)	Ai	47	80	74	81	73	–	–
Fedele et al. 1992 (39)	Ad	–	87	98	74	98	–	–
Reinhold et al. 1995 (29)	Ai	29	86	86	71	94	–	–
Huang et al. 1995 (40)	Ad	20	80	94	86	91	–	–
Atri et al. 1996 (11)	Ai	29	81	71	90	54	–	–
Reinhold et al.1996 (9)	Ai	24	89	89	71	96	–	–
Bazot et al. 2001 (11)	Ai	33	65	98	93	89	–	–
Bazot et al. 2002a (22)	Ai	91	81	100	100	40	–	–
Bazot et al. 2002b (22)	Ai	25	38	98	83	83	–	–
Kepkep et al. 2007 (26)	Ai	37	81	61	53	88	–	–
Meredith et al. 2009 (31)[a]	Ai	28[a]	83[a]	85[a]	–	–	4.7[a]	0.2[a]
Champaneria et al. 2010 (32)[a]	Ai	–	72[a]	81[a]	–	–	3.7[a]	0.3[a]
Sun et al. Taiwan 2010 (27)	Ai	40	87	60	59	88	–	–
Exacoustos et al. 2011 (28)	Ai	44	75/91	90/88	86/85	82/92	7.5	0.11
Andres et al. 2017 (35)[a]	Ai	–	83[a]	64[a]	–	–	–	–
MRI								
Reinhold et al. 1996 (9)	Ai	24	86	86	71	96	–	–
Bazot et al. 2001 (11)	Ai	33	78	93	84	89	–	–
Dueholm et al. 2001 (12)	Ai	21	64	88	58	90	5.3	0.4
Bazot et al. 2001 (56)	Ai	43	75/50/50	91/81/91	86/67/86	83/68/71		
Champaneria et al. 2010 (32)[a]	Ai	–	77[a]	89[a]	–	–	6.5[a]	0.2[a]

Note: Ad = adenomyoma; Ae = external adenomyosis; Ai = internal adenomyosis; MRI = magnetic resonance imaging; NLR = negative likelihood ratio; NPV = negative predictive value; PLR = positive likelihood ratio; PPV = positive predictive value; Prev = prevalence; Sens = sensitivity; Spec = specificity; US = ultrasound.
[a] Results from meta-analysis.

Bazot. Adenomyosis and imaging techniques. Fertil Steril 2018.

FIGURE 2

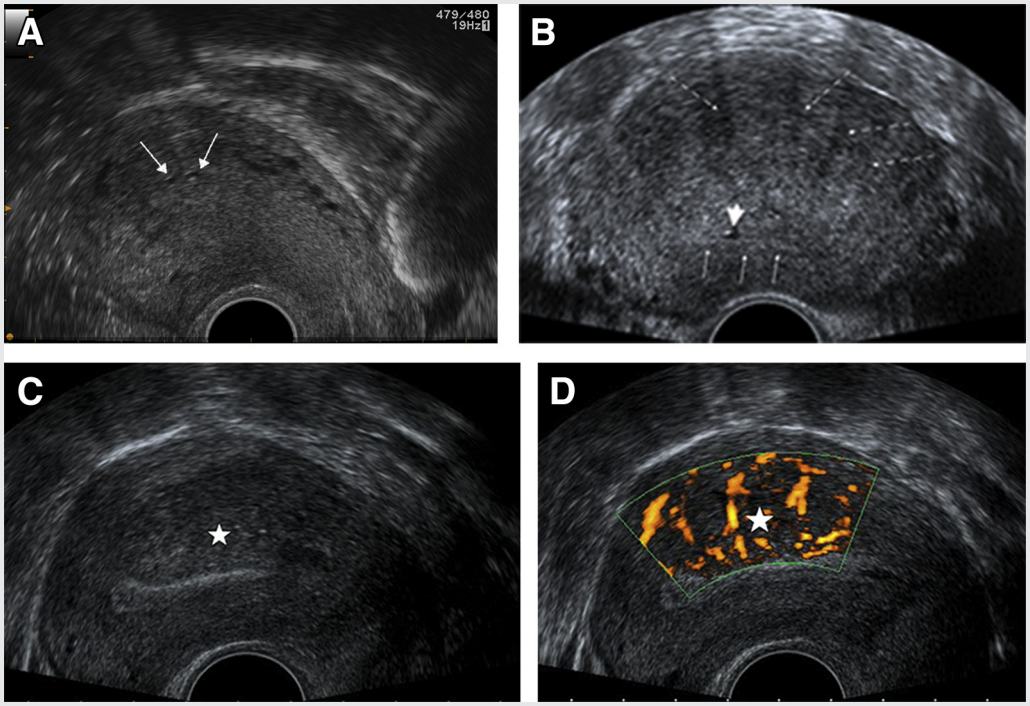

Transvaginal sonographic examinations in different patients showing (**A**) tiny subendometrial cysts (*arrows*) related to focal internal adenomyosis; (**B**) regular enlarged asymmetric heterogeneous myometrium containing multiple hypoechoic striations (*dotted arrows*), tiny myometrial cystic (*short arrow*) adjacent to poor definition of the endometrial-myometrial interface (*thin arrows*) related to diffuse adenomyosis; and (**C, D**) large posterior hypoechoic myometrial area (*star*) containing vessels following their course perpendicular to the endometrial interface due to diffuse adenomyosis.

Bazot. Adenomyosis and imaging techniques. Fertil Steril 2018.

sensitivities, pooled specificities and pooled positive likelihood ratios of 0.72–0.82, 0.85–0.81, and 4.67–3.7, respectively (31, 32). However, the most recent meta-analysis suggests that the heterogeneity between the studies is too great to allow statistical data pooling (23).

New US techniques are emerging and show promising results for the diagnosis of adenomyosis. Color or power Doppler US is useful to rule out the involvement of vascular structures (22). In the presence of features mimicking leiomyomas, power Doppler US displaying vessels perpendicular to the endometrial interface, is suggestive of adenomyosis (Fig. 2C and D) (33).

Two previous studies suggest that reconstructed three-dimensional TVS images provide superior visualization of the junctional zone (JZ) on the coronal section, facilitating analysis of the endomyometrial junction (28, 34). A recent meta-analysis suggested there was no improvement in overall accuracy in TVUS three-dimensional compared to TVUS two-dimensional for the diagnosis of adenomyosis (35).

Elastography is another emerging US technique and uses slight external tissue compression to quantify the strain produced in the structures examined (36). Two recent studies suggest significant differences in strain distribution between adenomyosis and leiomyomas (36, 37).

Transvaginal Sonography and External Adenomyosis

In a preliminary study including six women with suspected bladder endometriosis, TVS revealed an infiltration of the entire thickness of the bladder wall that was continuous with a nodule of adenomyosis of the anterior uterine wall in three of them (38).

To the best of our knowledge, no publications describe the role of TVS in the detection of posterior external adenomyosis. Sonographers should bear in mind that this subtype is particularly difficult to detect and that diagnosis should always be considered, especially in the presence of posterior deep endometriosis (18). In our experience, the outer posterior myometrial border appears heterogeneous on power Doppler analysis and can be seen to contain myometrial cysts and radial vessels (18).

Transvaginal Sonography and Adenomyomas

An adenomyoma appears on TVS as an ill-defined heterogeneous myometrial lesion containing hypoechoic spaces larger than 5 mm (39, 40). With these criteria, TVS has a sensitivity of between 80%–87% and a specificity of between 94%–98% (39, 40) (Table 2).

Occasionally, TVS suggests a submucosal adenomyoma in the presence of an ill-defined endometrial mass containing cystic lesions protruding into the endometrial cavity. Whatever its location, the differential diagnostic criteria with a leiomyoma are ill-defined margins and a cystic component (40). The absence of vascularization, or peripheral vascularization, on color Doppler sonography reinforces the diagnosis.

MRI AND ADENOMYOSIS

MRI is a second-line examination in the diagnosis of internal adenomyosis, mainly after a non-conclusive US evaluation. In addition, MRI can differentiate between the subtypes of adenomyosis.

MRI and Internal Adenomyosis

Several MRI diagnostic criteria, both direct and indirect, have been described based on the presence of endometrial glands (adeno) within the myometrium and smooth muscle cell hypertrophy (myosis) (9, 11, 12, 41) (Table 2). However, these criteria should not be used unless the radiologist has expert knowledge of uterine anatomy by MRI.

Most publications focusing on MRI highlight indirect rather than direct MRI criteria mainly due to the nice visualization of zonal anatomy of the uterus provided on MR imaging compared to anatomicohistologic methods (42). Several studies have analyzed the zonal anatomy of the uterus on T2-weighted imaging (43–49). It is composed of the JZ (displayed by a distinct inner low signal area), which separates the central endometrium (high signal intensity) from the outer myometrium (intermediate signal) (43).

Other authors have reported that the zonal anatomy is also visible on T1-weighted MRI with the JZ displayed as an inner high signal area, separating the central endometrium (low signal intensity), and the outer myometrium (intermediate signal) (50). In our experience, this zonal anatomy is best visualized on fat-suppressed T1-weighted MRI (18). The low signal intensity of JZ on T2-weighted MRI is related to its reduced T2 while the brightness on T1-weighted MRI is due to its reduced T1 (44, 50).

The knowledge of physiological variations of JZ and of its normal values is crucial for the diagnosis of internal adenomyosis (49). For example, the visualization of JZ is dependent on the patient's age and hormonal factors (51). It is not clearly depicted during premenarche, pregnancy, menopause, and in women on GnRH analogues (49). In contrast, visualization of the JZ can reappear in menopausal women taking hormone replacement therapy (49).

The most striking physiological modification of JZ is observed during menstruation when a pseudo-thickening of JZ is frequently observed (52). Hence, MRI evaluation of internal adenomyosis should always take into account the menstrual cycle and not be performed during the menstruation period if possible (18).

Both the endometrium and JZ (the archimyometrium) are of müllerian origin while the outer myometrium is of non-müllerian mesenchymal origin (53). The JZ plays a major role in uterine peristalsis (53). Normal uterine peristalsis is a continuous cyclic phenomenon and needs to be differentiated from uterine contractions.

Uterine contractions are sporadic, unpredictable, and usually spontaneously reversible within a few minutes (54, 55). They can be isolated or multiple, focal, or diffuse, and give rise to hypointense areas on T2-weighted MRI mimicking focal or diffuse internal adenomyosis, adenomyoma or leiomyoma. The use of rapid T2-weighted MR sequences is useful to identify spontaneous modifications or disappearance over time (56).

The definition of a normal JZ thickness is elusive and raises concerns about its evaluation. It has been regularly revised over the past three decades (9, 44, 46, 47, 50, 57) with the earlier studies giving a maximum threshold for normal JZ thickness at between 5 mm and 8 mm (44, 46, 47, 50, 57).

For many years, it was held that the most important MRI criterion to assess a diagnosis of adenomyosis was a maximal JZ thickness (JZ_{max}) $\geq$12 mm (9). This criterion, obtained by receiver operating characteristic analysis in Reinhold et al.'s study (9), was associated with a sensitivity and a specificity of 93% and 91%, respectively. However, two prospective studies evaluating this JZ_{max} value of $\geq$12 mm found lower sensitivities (63%–70%) and specificities (88%–96%) (11, 12). This discrepancy could partly be explained by differences in patient selection, especially with the exclusion of those with large leiomyomas in the study by Reinhold et al. (9).

In our experience, the JZ_{max} alone should be used with caution to diagnose internal adenomyosis (18). Limitations include the fact that in some patients the JZ is not visible and in others it may not be distinguishable from the outer myometrium. Moreover, JZ is not measurable in 20%–30% of women of reproductive age and in up to 50% of menopausal women (11, 58).

The presence of leiomyomas can also render JZ measurements difficult or impossible (11, 12, 41). In their series, Reinhold et al. (9) failed to identify any patients with adenomyosis and a non-measurable JZ (9). This could partly be explained by the exclusion of 28 patients for technical reasons (9).

Togashi et al. (8) suggested that a localized or diffuse thickening of the JZ was suggestive of adenomyosis (Fig. 3A) (8). However, it remains unclear whether focal thickening is related to a real disease or an epiphenomenon. A localized or focal JZ thickening is most commonly related to the presence of sporadic uterine contractions or leiomyoma rather than to adenomyosis (52).

Finally, most authors consider that JZ measurement should be made on a midsagittal T2-weighted MRI through the long axis of the uterus (Fig. 3B) (9, 41, 59). However, to diagnose internal adenomyosis it may be more useful to compare 3DT2-weighted MRI sequences with 2DT2-weighted MRI sequences to determine the JZ_{max}. The JZ_{max} thickness could also be evaluated by fat-sat suppressed T1-weighted MRI to determine its potential additional diagnostic value (18).

Other indirect MRI criteria have been evaluated for the diagnosis of internal adenomyosis (8, 9, 11, 12, 60). These include the ratio of JZ_{max} over the full myometrium thickness measured at the same place ($ratio_{max}$), the difference in maximal and minimal thicknesses in both anterior and posterior portions of the uterus (JZ differential = JZ_{diff}) and the presence of a big smooth regular uterus (9, 11, 12).

A significant difference has been found in the $ratio_{max}$ between patients with adenomyosis and a control group but without a clear threshold or with a $ratio_{max}$ of 40% giving rise to a sensitivity of 65% and a specificity of 93% in the diagnosis of internal adenomyosis (9, 11). Dueholm et al. suggested that a JZ_{diff} >5 mm was able to diagnose internal adenomyosis with a sensitivity and specificity of 70% and 85%, respectively (12). Finally, the presence of a big smooth regular uterus had poor sensitivity (23%) for the presence of internal adenomyosis but was highly specific (98%) (11). In contrast to common opinion, none of these indirect features used alone, including a JZ_{max} $\geq$12 mm, would appear to be sufficient to diagnose internal adenomyosis. In our experience, a combination of indirect criteria would be recommended to suggest adenomyosis (JZ_{max} $\geq$12 mm and/or $ratio_{max}$ >40% and/or big regular uterus) (11, 18). It is thus necessary to define direct criteria.

The main direct criterion for adenomyosis on MRI is the detection of tiny myometrial cysts related to islets of dilated ectopic endometrium (Fig. 3). These high-intensity myometrial foci ($\leq$3 mm) are embedded within the myometrium, most commonly in the inner myometrium, and display a high signal on T2 and a low signal on T1-weighted MRI (8, 9, 11, 12, 60). However, myometrial cysts, although almost always pathognomonic of adenomyosis, are detected in only about half of the cases on T2 (9, 11). This low sensitivity (~50%) is mainly due to the limited spatial resolution of 2D FSE T2-weighted MRI.

The prevalence of adenomyosis was found to be 39% overall in a study comparing in-vivo and ex-vivo pelvic MRI of 79 women (18). High-signal intensity myometrial

FIGURE 3

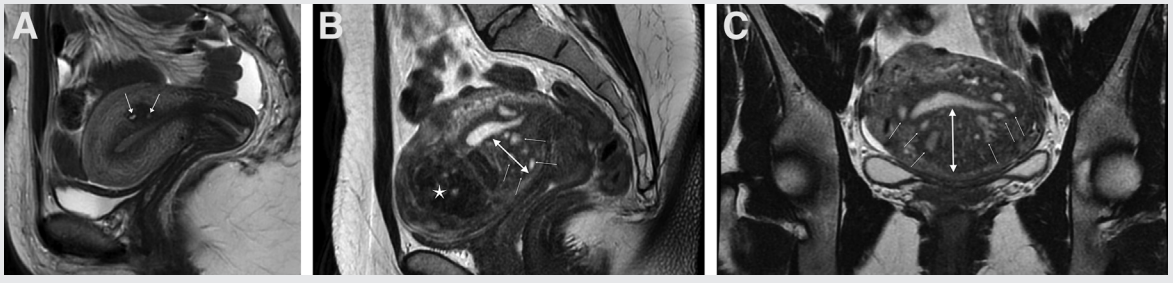

2DT2-weighted magnetic resonance imaging examinations of two different women. (**A**) A normal uterus with localized high intense tiny cystic component (*arrows*) surrounded by ill-defined low intense myometrial mass related to focal internal adenomyosis; (**B**) a huge uterus containing multiple cystic myometrial cysts with anterior diffuse thickening of junctional zone (*double arrow*) on sagittal view; and (**C**) coronal view related to diffuse internal adenomyosis with associated leiomyomas (*star*).

Bazot. Adenomyosis and imaging techniques. Fertil Steril 2018.

spots were visible on T2-weighted MRI in 50% of in-vivo cases and 90% of ex-vivo cases (18). This marked increase of sensitivity with unchanged specificity (98%-94%) can partly be explained by the absence of movement artifacts and a significant increase of spatial resolution with a pixel size of 0.87 × 1.27 in vivo and 0.56 × 0.56 ex vivo (18).

An upgrade of MR sequences and pelvic phased arrays is required to improve image quality and spatial resolution, namely by 3D FSE T2-weighted MRI. Increased susceptibility MRI sequences may also increase the detection of hemorrhagic foci as T1 and fat-suppressed T1-weighted imaging only detect hemorrhagic content within cystic cavities in <20% of cases (hyperintense signal).

Only three large prospective studies have compared MRI performance with histopathology for the diagnosis of adenomyosis (9, 11, 12). These studies give a sensitivity of between 70% to 93% and a specificity of 86–93%, with a prevalence of adenomyosis of 21 to 33% (9, 11, 12).

In their meta-analysis comparing the diagnostic performance of MRI and TVS, Champaneria et al. (32) reported that MRI had a pooled sensitivity of 77% (95% confidence interval [CI] 67–85), specificity of 89% (95% CI 84–92), a positive likelihood ratio of 6.5 (95% CI 4.5–9.3), and a negative likelihood ratio of 0.2 (95% CI 0.1–0.4) (32). The authors concluded that MRI performs more favorably than TVS in the presence of associated uterine leiomyomas (32).

However, while MRI is less operator dependent than TVS, expertise is required. Furthermore, breath-hold T2-weighted sequences in addition to conventional 2D TSE-T2-weighted MR sequences optimize the accuracy of MRI and reduce inter-observer variability (56, 61).

Few data are available on the value of MRI to determine the location, severity and extent of internal adenomyosis (9, 11). On histology, the extent of adenomyosis is estimated by the depth of penetration, the relative proportion of the uterus involved, and the weight of the uterus (62).

MR Imaging and External Adenomyosis

Several MRI characteristics should always be kept in mind for the diagnosis of external adenomyosis. First, external adenomyosis arises in the outer part of the uterus disrupting the serosa but not affecting the JZ (17). Second, it is quite always associated with deep endometriosis which appears to be the progenitor of this adenomyosis subtype (17). Third, the posterior myometrium is the most frequent location in line with the high frequency of posterior deep endometriosis (90%) (63, 64). Fourth, anterior external adenomyosis is a rare event (<8%) associated with the vesico-uterine fold, bladder involvement or round ligament endometriosis (64). Finally, external adenomyosis can be isolated or found in association with internal adenomyosis or adenomyomas.

On MRI, external adenomyosis is diagnosed as an ill-defined subserosal posterior or anterior myometrial mass giving a hypointense signal on T2-weighted MRI. This lesion often contains high-intensity central cystic areas visible on T2- and sometimes on T1-weighted MRI (Fig. 4). In the absence of associated internal adenomyosis, the JZ is not affected. No specific data have been published to evaluate the performance of MRI for the diagnosis of external adenomyosis, probably because this entity is rarely distinguished from deep endometriosis.

MR Imaging and Adenomyomas

An adenomyoma is diagnosed as an ill-defined myometrial mass that is hypointense on T2-weighted MRI. This lesion always contains high-intensity central cystic areas visible on T2- and sometimes on T1-weighted MRI (65–67). Neither the JZ nor the uterine serosa is affected in the presence of an isolated adenomyoma (17). MRI is accurate in depicting their location (intramural, submucosal, or subserosal), number, and potential association with internal adenomyosis or leiomyomas.

Pitfalls in the diagnosis of adenomyoma include leiomyomas and myometrial contractions. Sustained myometrial contraction is represented by focal or diffuse sporadic bulging of the myometrium into the uterine cavity. Uterine contractions can be differentiated from adenomyoma or leiomyoma on sequential studies by their transient nature (52).

Cystic adenomyoma is characterized by its predominant hemorrhage content. On MRI, cystic adenomyomas display

FIGURE 4

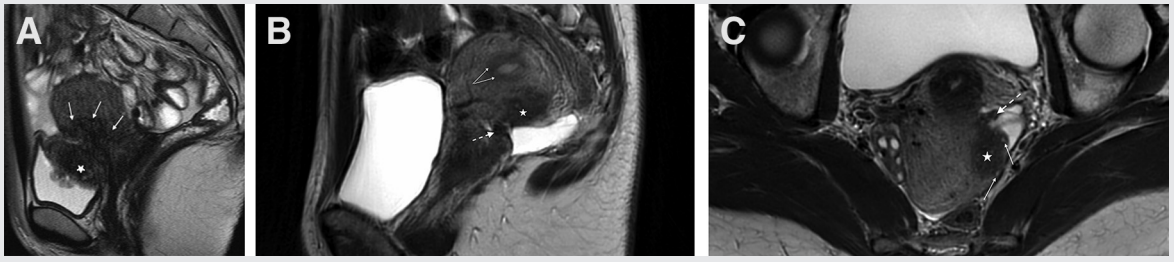

T2-weighted magnetic resonance imaging examinations in two different women. (**A**) A large low intense ill-defined mass invading bladder wall, vesicouterine pouch, and adjacent anterior myometrium related to bladder endometriosis (*star*) with anterior external adenomyosis (*arrows*); (**B**) retroflexed uterus presenting with normal junctional zone on sagittal view (*double arrow*); and (**C**) large posterior ill-defined low signal intense mass (*star*) containing tiny cystic component (*thin arrow*) on axial oblique view associated with uterosacral ligament thickening (*dotted arrow*) related to posterior deep endometriosis and posterior external adenomyosis.

Bazot. Adenomyosis and imaging techniques. Fertil Steril 2018.

homogeneously high signal intensity on T1-weighted MRI (68). The appearance on T2-weighted MRI is variable reflecting hemorrhage in different stages of organization (68). In addition, fluid-fluid level and low signal rim on T2 are sometimes present (68). In adult women, the main differential diagnosis is represented by leiomyoma in red degeneration histology. Cystic adenomyoma is also sometimes discovered in young women being responsible of severe chronic pelvic pain and mimics uterine anomalies (69, 70).

In conclusion, the diagnosis of adenomyosis remains a major challenge for imaging techniques. Our analysis suggests that MRI is more useful than TVS in the diagnosis of adenomyosis. Further studies are required to evaluate whether 3T MRI could improve performance. From a clinical point of view, consensus is required to adopt a classification of adenomyosis with the aim not only of improving reproducibility but also the prediction of therapeutic response and prognosis.

Acknowledgments: The authors thank Ani and Hasmik Koulakian for creating drawings in accordance with our proposed classification.

REFERENCES

1. Zaloudek C, Hendrickson MR. Mesenchymal tumors of the uterus. In: Kurman RJ, editor. Blaustein's pathology of the female genital tract 1. New York: Springer-Verlag; 2002:561–615.
2. Molitor JJ. Adenomyosis: a clinical and pathologic appraisal. Am J Obstet Gynecol 1971;110:275–84.
3. Bird CC, Mc Elin TW, Manalo-Estrella P. The elusive adenomyosis of the uterus-revisited. Am J Obstet Gynecol 1972;112:583–93.
4. Siegler AM, Camillien L. Adenomyosis. Clinical perspectives. J Reprod Med 1994;39:841–53.
5. Leyendecker G, Wildt L, Mall G. The pathophysiology of endometriosis and adenomyosis: tissue injury and repair. Arch Gynecol Obstet 2009; 280:529–38.
6. Benagiano G, Habiba M, Brosens I. The pathophysiology of uterine adenomyosis: an update. Fertil Steril 2012;98:572–9.
7. Guo SW, Mao X, Ma Q, Liu X. Dysmenorrhea and its severity are associated with increased uterine contractility and overexpression of oxytocin receptor (OTR) in women with symptomatic adenomyosis. Fertil Steril 2013;99:231–40.
8. Togashi K, Nishimura K, Itoh K, Fujisawa I, Noma S, Kanaoka M, et al. Adenomyosis: diagnosis with MR imaging. Radiology 1988;166:111–4.
9. Reinhold C, McCarthy S, Bret PM, Mehio A, Atri M, Zakarian R, et al. Diffuse adenomyosis: comparison of endovaginal US and MR imaging with histopathologic correlation. Radiology 1996;199:151–8.
10. Atri M, Reinhold C, Mehio AR, Chapman WB, Bret PM. Adenomyosis: US features with histologic correlation in an in-vitro study. Radiology 2000; 215:783–90.
11. Bazot M, Cortez A, Darai E, Rouger J, Chopier J, Antoine JM, et al. Ultrasonography compared with magnetic resonance imaging for the diagnosis of adenomyosis: correlation with histopathology. Hum Reprod 2001;16:2427–33.
12. Dueholm M, Lundorf E, Hansen ES, Sorensen JS, Ledertoug S, Olesen F. Magnetic resonance imaging and transvaginal ultrasonography for the diagnosis of adenomyosis. Fertil Steril 2001;76:588–94.
13. Gordts S, Brosens JJ, Fusi L, Benagiano G, Brosens I. Uterine adenomyosis: a need for uniform terminology and consensus classification. Reprod Biomed Online 2008;17:244–8.
14. Rokitansky C. Über Uterusdrüsen-neudildung in uterus and ovarial-sarcomen. Zeitsch Gesellschaft der Aerzte in Wien 1860;16:577–81.
15. Cullen TS. The distribution of adenomyomas containing uterine mucosa. Arch Surg 1920;1:215–83.
16. Sampson JA. Perforating hemorrhagic (chocolate) cysts of the ovary. Their importance and especially their relation to pelvic adenomas of endometrial type. Adenomyoma of the uterus, rectovaginal septum, sigmoid, etc. Arch Surg 1921;3:245–323.
17. Kishi Y, Suginami H, Kuramori R, Yabuta M, Suginami R, Taniguchi F. Four subtypes of adenomyosis assessed by magnetic resonance imaging and their specification. Am J Obstet Gynecol 2012;207:114.e1–7.
18. Bazot M. Pathologie myométriale. In: Nahum H, editor. Imagerie de la femme–Gynécologie. 2. Paris: Lavoisier; 2017.
19. Gordts S, Grimbizis GF, Campo R. Symptoms and classification of uterine adenomyosis including the place of hysteroscopy in diagnosis. Fertil Steril 2018;109:380–8.
20. Walsh JW, Taylor KJ, Rosenfield AT. Gray scale ultrasonography in the diagnosis of endometriosis and adenomyosis. AJR Am J Roentgenol 1979;132: 87–90.
21. Siedler D, Laing FC, Jeffrey RB Jr, Wing VW. Uterine adenomyosis. A difficult sonographic diagnosis. J Ultrasound Med 1987;6:34–9.
22. Bazot M, Darai E, Rouger J, Detchev R, Cortez A, Uzan S. Limitations of transvaginal sonography for the diagnosis of adenomyosis, with histopathological correlation. Ultrasound Obstet Gynecol 2002;20:605–11.
23. Dartmouth K. A systematic review with meta-analysis: the common sonographic characteristics of adenomyosis. Ultrasound 2014;22:148–57.
24. Van den Bosch T, Dueholm M, Leone FP, Valentin L, Rasmussen CK, Votino A, et al. Terms, definitions and measurements to describe sonographic features of myometrium and uterine masses: a consensus opinion from the Morphological Uterus Sonographic Assessment (MUSA) group. Ultrasound Obstet Gynecol 2015;46:284–98.
25. Fedele L, Bianchi S, Dorta M, Arcaini L, Zanotti F, Carinelli S. Transvaginal ultrasonography in the diagnosis of diffuse adenomyosis. Fertil Steril 1992;58:94–7.
26. Kepkep K, Tuncay YA, Goynumer G, Tutal E. Transvaginal sonography in the diagnosis of adenomyosis: which findings are most accurate? Ultrasound Obstet Gynecol 2007;30:341–5.
27. Sun YL, Wang CB, Lee CY, Wun TH, Lin P, Lin YH, et al. Transvaginal sonographic criteria for the diagnosis of adenomyosis based on histopathologic correlation. Taiwan J Obstet Gynecol 2010;49:40–4.
28. Exacoustos C, Brienza L, Di Giovanni A, Szabolcs B, Romanini ME, Zupi E, et al. Adenomyosis: three-dimensional sonographic findings of the junctional zone and correlation with histology. Ultrasound Obstet Gynecol 2011;37:471–9.
29. Reinhold C, Atri M, Mehio A, Zakarian R, Aldis AE, Bret PM. Diffuse uterine adenomyosis: morphologic criteria and diagnostic accuracy of endovaginal sonography. Radiology 1995;197:609–14.
30. Hulka CA, Hall DA, McCarthy K, Simeone J. Sonographic findings in patients with adenomyosis: can sonography assist in predicting extent of disease? AJR Am J Roentgenol 2002;179:379–83.
31. Meredith SM, Sanchez-Ramos L, Kaunitz AM. Diagnostic accuracy of transvaginal sonography for the diagnosis of adenomyosis: systematic review and metaanalysis. Am J Obstet Gynecol 2009;201:107.e1–6.
32. Champaneria R, Abedin P, Daniels J, Balogun M, Khan KS. Ultrasound scan and magnetic resonance imaging for the diagnosis of adenomyosis: systematic review comparing test accuracy. Acta Obstet Gynecol Scand 2010;89: 1374–84.
33. Perrot N, Frey I, Mergui JL, Bazot M, Uzan M, Uzan S. Picture of the month. Adenomyosis: power Doppler findings. Ultrasound Obstet Gynecol 2001; 17:177–8.
34. Luciano DE, Exacoustos C, Albrecht L, Lamonica R, Proffer A, Zupi E, et al. Three-dimensional ultrasound in diagnosis of adenomyosis: histologic correlation with ultrasound targeted biopsies of the uterus. J Minim Invasive Gynecol 2013;20:803–10.
35. Andres MP, Borrelli GM, Ribeiro J, Baracat EC, Abrao MS, Kho RM. Transvaginal ultrasound for the diagnosis of adenomyosis: systematic review and meta-analysis. J Minim Invasive Gynecol 2018;25:257–64.
36. Tessarolo M, Bonino L, Camanni M, Deltetto F. Elastosonography: a possible new tool for diagnosis of adenomyosis? Eur Radiol 2011;21:1546–52.
37. Frank ML, Schafer SD, Mollers M, Falkenberg MK, Braun J, Mollmann U, et al. Importance of Transvaginal elastography in the diagnosis of uterine fibroids and adenomyosis. Ultraschall Med 2016;37:373–8.

38. Fedele L, Piazzola E, Raffaelli R, Bianchi S. Bladder endometriosis: deep infiltrating endometriosis or adenomyosis? Fertil Steril 1998;69:972–5.
39. Fedele L, Bianchi S, Dorta M, Zanotti F, Brioschi D, Carinelli S. Transvaginal ultrasonography in the differential diagnosis of adenomyoma versus leiomyoma. Am J Obstet Gynecol 1992;167:603–6.
40. Huang RT, Chou CY, Chang CH, Yu CH, Huang SC, Yao BL. Differentiation between adenomyoma and leiomyoma with transvaginal ultrasonography. Ultrasound Obstet Gynecol 1995;5:47–50.
41. Novellas S, Chassang M, Delotte J, Toullalan O, Chevallier A, Bouaziz J, et al. MRI characteristics of the uterine junctional zone: from normal to the diagnosis of adenomyosis. AJR Am J Roentgenol 2011;196:1206–13.
42. Fusi L, Cloke B, Brosens JJ. The uterine junctional zone. Best Pract Res Clin Obstet Gynaecol 2006;20:479–91.
43. Hricak H, Alpers C, Crooks LE, Sheldon PE. Magnetic resonance imaging of the female pelvis: initial experience. AJR Am J Roentgenol 1983;141:1119–28.
44. Lee JK, Gersell DJ, Balfe DM, Worthington JL, Picus D, Gapp G. The uterus: in vitro MR-anatomic correlation of normal and abnormal specimens. Radiology 1985;157:175–9.
45. McCarthy S, Tauber C, Gore J. Female pelvic anatomy: MR assessment of variations during the menstrual cycle and with use of oral contraceptives. Radiology 1986;160:119–23.
46. Brown HK, Stoll BS, Nicosia SV, Fiorica JV, Hambley PS, Clarke LP, et al. Uterine junctional zone: correlation between histologic findings and MR imaging. Radiology 1991;179:409–13.
47. Scoutt LM, Flynn SD, Luthringer DJ, McCauley TR, McCarthy SM. Junctional zone of the uterus: correlation of MR imaging and histologic examination of hysterectomy specimens. Radiology 1991;179:403–7.
48. Scoutt LM, McCauley TR, Flynn SD, Luthringer DJ, McCarthy SM. Zonal anatomy of the cervix: correlation of MR imaging and histologic examination of hysterectomy specimens. Radiology 1993;186:159–62.
49. Brosens JJ, de Souza NM, Barker FG. Uterine junctional zone: function and disease. Lancet 1995;346:558–60.
50. McCarthy S, Scott G, Majumdar S, Shapiro B, Thompson S, Lange R, et al. Uterine junctional zone: MR study of water content and relaxation properties. Radiology 1989;171:241–3.
51. Kiguchi K, Kido A, Kataoka M, Shitano F, Fujimoto K, Himoto Y, et al. Uterine peristalsis and junctional zone: correlation with age and postmenopausal status. Acta Radiol 2017;58:224–31.
52. Tamai K, Togashi K, Ito T, Morisawa N, Fujiwara T, Koyama T. MR imaging findings of adenomyosis: correlation with histopathologic features and diagnostic pitfalls. Radiographics 2005;25:21–40.
53. Brosens JJ, Barker FG, de Souza NM. Myometrial zonal differentiation and uterine junctional zone hyperplasia in the non-pregnant uterus. Hum Reprod Update 1998;4:496–502.
54. Togashi K, Kawakami S, Kimura I, Asato R, Takakura K, Mori T, et al. Sustained uterine contractions: a cause of hypointense myometrial bulging. Radiology 1993;187:707–10.
55. Masui T, Katayama M, Kobayashi S, Shimizu S, Nozaki A, Sakahara H. Pseudolesions related to uterine contraction: characterization with multiphase-multisection T2-weighted MR imaging. Radiology 2003;227:345–52.
56. Bazot M, Darai E, Clement de Givry S, Boudghene F, Uzan S, Le Blanche AF. Fast breath-hold T2-weighted MR imaging reduces interobserver variability in the diagnosis of adenomyosis. AJR Am J Roentgenol 2003;180:1291–6.
57. Kang S, Turner DA, Foster GS, Rapoport MI, Spencer SA, Wang JZ. Adenomyosis: specificity of 5 mm as the maximum normal uterine junctional zone thickness in MR images. AJR Am J Roentgenol 1996;166:1145–50.
58. de Souza NM, Brosens JJ, Schwieso JE, Paraschos T, Winston RM. The potential value of magnetic resonance imaging in infertility. Clin Radiol 1995;50:75–9.
59. Masui T, Katayama M, Kobayashi S, Nakayama S, Nozaki A, Kabasawa H, et al. Changes in myometrial and junctional zone thickness and signal intensity: demonstration with kinematic T2-weighted MR imaging. Radiology 2001;221:75–85.
60. Togashi K, Ozasa H, Konishi I, Itoh H, Nishimura K, Fujisawa I, et al. Enlarged uterus: differentiation between adenomyosis and leiomyoma with MR imaging. Radiology 1989;171:531–4.
61. Krinsky G, DeCorato DR, Rofsky NM, Flyer M, Earls JP, Ambrosino M, et al. Rapid T2-weighted MR imaging of uterine leiomyoma and adenomyosis. Abdom Imaging 1997;22:531–4.
62. Benson RC, Sneeden D. Adenomyosis: a reapraisal of symptomatology. Am J Obstet Gynecol 1958;76:1044–61.
63. Chapron C, Fauconnier A, Vieira M, Barakat H, Dousset B, Pansini V, et al. Anatomical distribution of deeply infiltrating endometriosis: surgical implications and proposition for a classification. Hum Reprod 2003;18:157–61.
64. Bazot M, Darai E, Hourani R, Thomassin I, Cortez A, Uzan S, et al. Deep pelvic endometriosis: MR imaging for diagnosis and prediction of extension of disease. Radiology 2004;232:379–89.
65. Yamashita Y, Torashima M, Hatanaka Y, Takahashi M, Fukumatsu K, Tanaka N, et al. MR imaging of atypical polypoid adenomyoma. Comput Med Imaging Graph 1995;19:351–5.
66. Byun JY, Kim SE, Choi BG, Ko GY, Jung SE, Choi KH. Diffuse and focal adenomyosis: MR imaging findings. Radiographics 1999;19 Spec No:S161–70.
67. Song SE, Sung DJ, Park BJ, Kim MJ, Cho SB, Kim KA. MR imaging features of uterine adenomyomas. Abdom Imaging 2011;36:483–8.
68. Troiano RN, Flynn SD, McCarthy S. Cystic adenomyosis of the uterus: MRI. J Magn Reson Imaging 1998;8:1198–202.
69. Takeuchi H, Kitade M, Kikuchi I, Kumakiri J, Kuroda K, Jinushi M. Diagnosis, laparoscopic management, and histopathologic findings of juvenile cystic adenomyoma: a review of nine cases. Fertil Steril 2010;94:862–8.
70. Dadhwal V, Sharma A, Khoiwal K. Juvenile cystic adenomyoma mimicking a uterine anomaly: a report of two cases. Eurasian J Med 2017;49:59–61.